Synthesis and Reactivity of s -Aryltetrazines Palladacycles Toward a Direct o -Aryl C–H Bond Halogenation Achieved by Electrocatalysis

Asmae Bousfiha, Sophie Fournier, Hélène Cattey, Paul Fleurat-Lessard, Charles Devillers, Dominique Lucas, Jean-Cyrille Hierso, Julien Roger

Synthesis and Reactivity of *s*-Aryltetrazines Palladacycles towards a Direct *o*-Aryl C–H Bond Halogenation Achieved by Electrocatalysis

Asmae Bousfiha, Sophie Fournier, Hélène Cattey, Paul Fleurat-Lessard, Charles H. Devillers, Dominique Lucas, Jean-Cyrille Hierso* and Julien Roger**

Université de Bourgogne, Institut de Chimie Moléculaire de l'Université de Bourgogne (ICMUB - UMR CNRS 6302), 9 avenue Alain Savary, 21078 Dijon Cedex, France

ABSTRACT: Electrocatalysis is considered a promising approach towards cleaner, precisely controlled, and low waste-producing transition metal-catalyzed C–H bond activation/functionalization. However, some useful redox active substrates could be challenging to use in electrocatalysis, depending on their redox potential and intrinsic reactivity. Accordingly, the topical *s*-aryltetrazines have not been employed, up to now, for their selective transition metal-promoted *ortho*-C–H functionalization using an electrocatalytic process. Herein, we addressed this challenging issue stepwisely by synthesizing first a series of stable and well-defined dinuclear and mononuclear palladacycles of the *s*-diphenyltetrazine. These compounds are considered as pertinent intermediates of direct C–H functionalization of *s*-aryltetrazines in a palladium-catalyzed approach. The palladium complexes were characterized by multinuclear NMR spectroscopy in solution, and single crystal X-ray diffraction analysis in the solid state. Their electrochemical behavior was established by cyclic voltammetry. We successfully achieved the reductive elimination of *o*-C–H halogenated *s*-diphenyltetrazine under electrochemical conditions from its corresponding mononuclear *o*-metallated *s*-aryltetrazine palladium halide, establishing the electrochemically controlled palladium-promoted *o*-C–H halogenation of a *s*-aryltetrazine.

From this elementary step achieved under electrocatalytic control, we devised simple conditions for effective electrochemical palladium-catalyzed C–H *ortho*-chlorination and iodination of *s*-aryltetrazines, using cheap lithium halide salt as nucleophile source. While these conditions still suffer from multiple halogenation reactions, and especially the symmetrical bis-halogenation, they open the way, as proof-of-concept, to unprecedented electrochemically controlled direct functionalization of the redox active *s*-aryltetrazines.

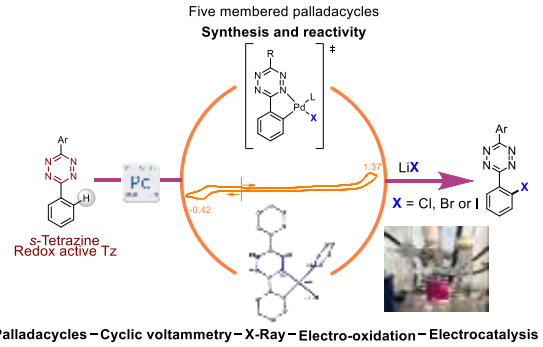

■ INTRODUCTION

Direct C–H functionalization catalyzed by transition metals has emerged as a useful synthetic tool to straightforwardly build functionalized (hetero)aryl compounds.[1,2] The extension to electrocatalytic C–H activation is considered as a promising powerful tool of molecular functionalization, in which electrochemistry could substitute the use of costly and toxic stoichiometric redox reagents,[3,4] and reduce the negative impact of classical thermal conditions on energy cost, sensitive substrates, high-boiling point solvents, etc. The ability to finely control the oxidative potential in a catalytic reaction is very attractive, instead of relying on the intrinsic potential of typically polluting or overacting chemical oxidants such as benzoquinone, $FeCl_3$, phenyl iodide diacetate (PIDA), expensive metal oxides (based on Cu, Ag, *etc.*) or even O_2. In general, the anodic oxidation process can take place either to oxidize an organometallic intermediate to a reactive high-valence species, or to regenerate the catalytic center at the end of a cycle. Accordingly, a variety of functional groups can be introduced on alkyl and (hetero)aryl substrates by the smart combination of a transition metal-catalyzed C–H activation and an electrochemical process, this leading to the efficient formation of C–C, C–O, C–P, C–N, C–halogen bonds, etc.[4]

Among the transition metals employed, palladium is one of the most frequently used in homogeneous conditions electrocatalysis because of its versatility and excellent tolerance to functional groups. However, while the *N*-directed palladium-catalyzed C–H halogenation has been extensively developed,[5] the related electrochemically-promoted approaches remain underdeveloped (Figure 1). Kakiuchi and co-workers reported the first example of a palladium-catalyzed C–H electrophilic halogenation of arylpyridine derivatives using hydrochloric or hydrobromic acid under the electrochemical oxidation of $PdCl_2$ or $PdBr_2$ in DMF to access Pd(IV) chemistry.[6] They successfully extended C–H chlorination and bromination to C–H iodination, using $PdOAc_2$ as the catalyst and iodine (I_2) or potassium iodide in order to generate the reactive species in acetonitrile.[7] This group also reported the bidentate ligand *N*-quinolinylbenzamide as the directing group to create new C–Cl or C–I bond under similar conditions. Hydrochloric acid was used as chlorinating agent in the presence of $PdCl_2$ as the catalyst.[8,9] More recently, Mei's group reported a bromination of benzamide derivatives, in which NH_4Br served both as brominating agent and electrolyte.[10]

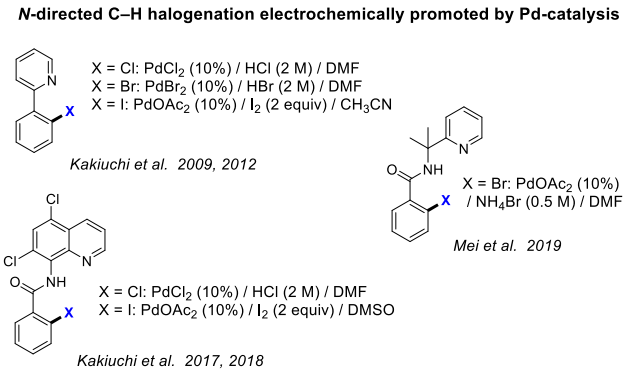

Figure 1. State-of-the art with conditions for electrochemically promoted *N*-ligand directed sp^2-C–H halogenation by palladium catalysis.

Based on the very broad field of applications of topical *s*-aryltetrazines,[11] our group recently developed a new synthetic route based on a *N*-*ortho*-directed strategy for the selective introduction of halides onto these sensitive substrates by transition metals.[12] We first established the compatibility between palladium C–H activation/functionalization catalysis and the redox tetrazine (Tz) core in the *ortho*-aryl-C–H direct halogenation of *s*-aryltetrazines using an electrophilic source (*N*-halosuccinimides, NXS, X = Cl, Br, I) or nucleophilic sources (LiX or NaX), which allowed further building of novel polyaromatic compounds.[12b,13] Herein, we addressed the challenging *ortho*-C–H electrocatalytic halogenation of *s*-diphenyltetrazine stepwisely, by synthesizing first a series of stable and well-defined dinuclear and mononuclear pertinent palladacycles, which are characterized by multinuclear NMR spectroscopy, X-ray diffraction analysis and by cyclic voltammetry. Then, we successfully achieved at room temperature, under electrochemical conditions, the reductive elimination of *o*-C–H halogenated *s*-diphenyltetrazine from its corresponding mononuclear *o*-metallated *s*-aryltetrazine palladium halide. Finally, we determined simple conditions for the effective electrochemical palladium-catalyzed C–H *ortho*-chlorination and iodination of *s*-aryltetrazines. This, by using a cheap, low-mass, lithium salt as the halogen source.

■ RESULTS AND DISCUSSION

The *s*-tetrazine core is an electron-poor nitrogen-based platform, easily reducible compared to many other heteroaromatics, including parent compounds such as pyridines or pyrazoles, that are typically used as valuable *N*-directing ligands for C–H functionalization. The *ortho*-functionalization of pristine *s*-diaryltetrazines is synthetically challenging since up to four identical C–H bonds can be functionalized; this generally requires an extensive screening of reaction conditions to improve, as much as possible, the selectivity.[12a] On the other hand, the tetrazine core being reversibly reduced in a one-electron process, it forms a radical anion that reacts in the presence of water.[11a] This redox response is a limitation in the electrocatalysis process that reduces the choice of the cell configuration, which thus requires also a fine control of the reactions occurring at the counter electrode.[3,4]

To overcome these limitations, we first focused on decoupling the C–H activation step from the electrochemical oxidation (Figure 2, top). Accordingly, we synthesized and characterized a series of di- and mononuclear palladacycles from *ortho*-metallation of the *s*-diphenyltetrazine **1**, which were isolated as potentially pertinent intermediates of the catalytic *o*-C–H functionalization (complexes **2**, **3-X**, **4** and **5**, Schemes 1-3).

Palladium complexes formation from *s*-diphenyltetrazine 1. Dimeric palladacycles have been previously identified as pertinent intermediates for the reductive elimination step towards C–C, C–O, C–N or C–halogen bond formation.[14] Still, during the genuine (*non-stoichiometric*) catalytic process, monomeric

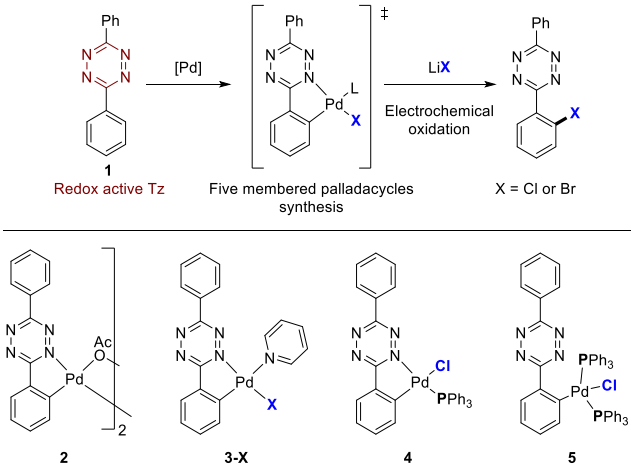

Figure 2. Stepwise approach to electrocatalyzed C–H halogenation of *s*-diphenyltetrazines (top). Palladium complexes formed from the *ortho*-metallation of *s*-diphenyltetrazine for electrochemical oxidation studies (bottom).

Scheme 1. Dimeric palladacycle of *s*-diphenyltetrazine (2).

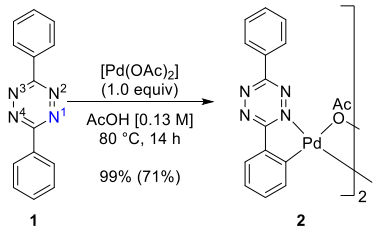

palladacycles were suggested to be the effective catalytic species, notably because of the much higher concentration of *N*-directing ligand and dissociating coordinating solvent.[15]

The dimeric cyclometallated palladium complex (**2**, Scheme 1) of the *s*-diphenyltetrazine **1** is formed in AcOH as the solvent at 80 °C.[16,15a,13] This dimeric palladacycle was isolated in 71% after precipitation by diffusion of *n*-heptane in a dichloromethane solution. The 2D ^{1}H NMR analysis of this compound justified the formation of only one isomer (**2**, Figure S-1 to S-3 in the Supporting Information).[17]

We specifically synthesized monomeric species by the addition of pyridine and phosphine to account for a second ligand in the coordination sphere of Pd.[12b,18] The monomeric palladacycles **3-X**, **4** and **5** was obtained by the introduction of an excess of ligands such as pyridine (Scheme 2) and triphenylphosphine (Scheme 3). Starting from the dimeric complex **2**, we first achieved an exchange from bridged acetate ligands to halide (X = Cl or Br) by the addition of 10 equiv. of the corresponding LiX salt in chloroform. Typically, these insoluble intermediates solubilized after the addition of 2 equiv. of pyridine in dichloromethane. The monomeric **3-Cl** was isolated in 61% after crystallization by diffusion of *n*-heptane into a solution of dichloromethane. The brominated counterpart **3-Br** was isolated in 83% yield using LiBr. The iodinated **3-I** could not be isolated in a pure form. Single crystals of **3-Cl** were analyzed by X-ray diffraction (Figure 3), establishing in the solid state the metallacycle formation. The structure shows a distorted square-planar environment for the palladium center (see for instance, the constrained angle C1–Pd1–N1=81.54(7) °), in which the chlorine and the donor-nitrogen atom are in a *trans*-mutual position.

Scheme 2. Synthesis of monomeric palladacycle of *s*-tetrazine (3-X, X = Cl, Br) with pyridine.

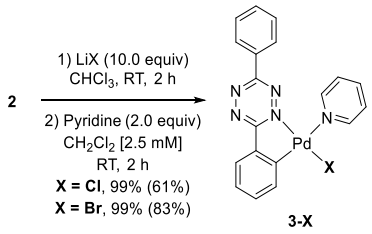

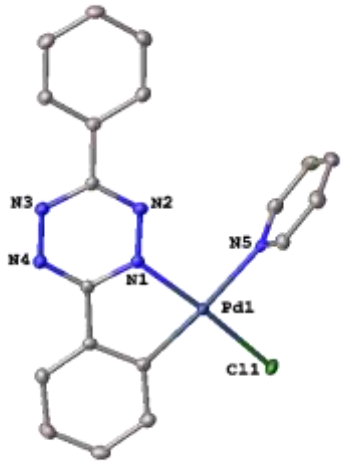

Figure 3. Molecular structures of **3-Cl**. Hydrogen atoms are omitted for clarity and only one independent molecule is shown. Selected bond lengths and distances (Å) and angles (deg): Pd1–C1=1.9900(17); Pd1–N1=2.0152(15); Pd1–N5=2.13336(15); Pd1–Cl1=2.3025(7); N1–Pd1–N5=93.23(6); N5–Pd1–Cl1=91.64(4); C1–Pd1–Cl1=93.76(5); C1–Pd1–N1=81.54(7); N1–Pd1–Cl1=173.84(4).

Scheme 3. Synthesis of monomeric palladacycle of *s*-tetrazine with triphenylphosphine.

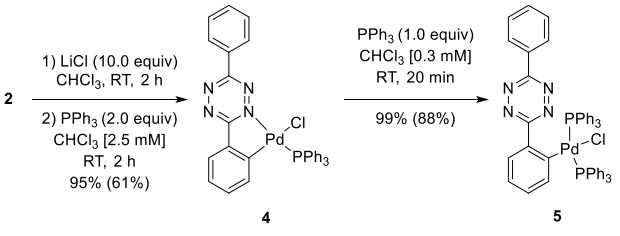

Following the same synthetic strategy, the introduction of triphenylphosphine as the ligand produced the complex **4** in 61% isolated yield after crystallization (Scheme 3). This complex was characterized by ^{31}P NMR signal located at 43 ppm. The evolution of **4** to a second diphosphinated palladium complex **5** was attested by a ^{31}P NMR signal shift at 23 ppm. The excess of phosphine and the higher nucleophilicity of phosphorus compared to nitrogen induced the formation of this complex after *N*-decoordination of the *s*-tetrazine core from the metal center.[19] The single crystal XRD analysis of the complexes **4** and **5** correlated the NMR solution analysis (Figure 4). We also achieved the quantitative formation of **5** that was isolated in 88% yield from **4** by the addition of one equivalent of PPh_3.

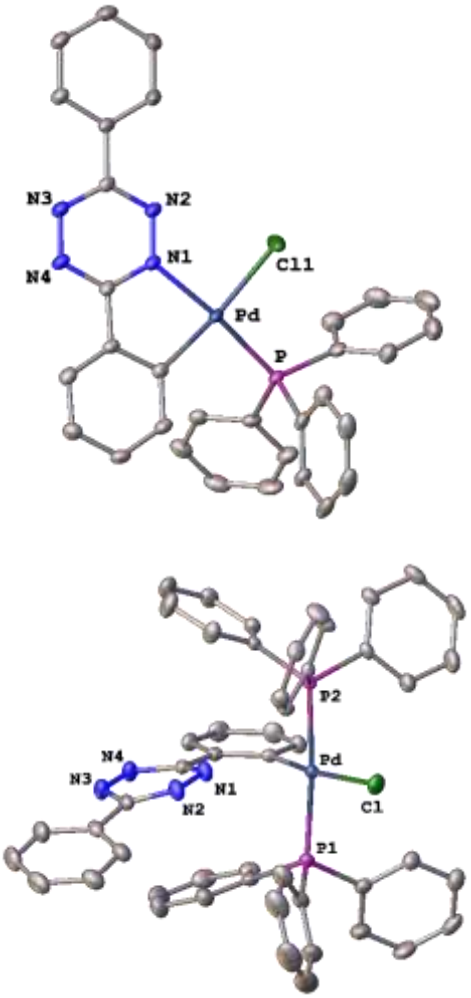

Figure 4. Molecular structures of **4** (top), and **5** (bottom). Hydrogen atoms are omitted for clarity. For **4**, one dichloromethane and for **5**, two methanol as solvent molecules were omitted. Selected bond lengths and distances (Å) and angles (deg). **4**: Pd–Cl1=2.3631(8); Pd–P=2.2610(7); Pd–N1=2.103(2); Pd–C1=2.030(3); P–Pd–Cl1=92.82(3); N1–Pd–Cl1=91.85(7); C1–Pd–N1=81.16(10); C1–Pd–P=94.86(8); N1–Pd–P=171.67(7). **5**: Pd–Cl=2.4076(4); Pd–P1=2.3197(5); Pd–P2=2.3194(5); Pd–C1=1.9975(16); C1–Pd–P1=89.71(5); C1–Pd–P2=86.54(5); P1–Pd–Cl=93.617(16); P2–Pd–Cl=90.648(15); P2–Pd–P1=175.032(16).

In the XRD structure of complex **4**, similarly to **3-Cl**, the geometry around the palladium center remains square-planar but is strongly distorted because of the C,N-chelation (see the angle C1–Pd–N1=81.16(10) °). However, in **4** the chlorine and the nitrogen atom are in a *cis*-mutual position. The XRD analysis of **5** confirmed the nitrogen-decoordination of the tetrazine core from the metal center, replaced by the second phosphine. This resulted in a more regular square-planar geometry around the palladium center where the mutual angles of ancillary ligands around Pd are comprised between 86.54(5) ° and 93.617(16) °. The phosphines groups are in a mutual *trans*-position.

Having isolated in pure form these palladacycles we examined their electrochemical behavior, especially to assess the compatibility of the tetrazine core with electrocatalytic conditions.

Electrochemical study of palladium complexes.

Cyclic voltammetry (CV). A CV study of the palladacycles and derivatives **2**, **3-X**, **4**, **5** and their precursor ligand **1** was performed in a DMF solution (10^{-3} M) with $TEABF_4$ as the supporting electrolyte (0.1 M), a glassy carbon disk working electrode and a saturated KCl calomel reference electrode (SCE) as the reference electrode (Table 1, Figures 5 and 6). The redox behaviour of the dinuclear and mononuclear palladacycle complexes were analyzed both in the oxidative and reductive potential scan directions.

Table 1. Oxidation and reduction peak potentials (V *vs* SCE) for the complexes **2**, **3-Cl**, **3-Br**, **4** and **5** from CV.

	oxidation		reduction		
complex	$E_p(O_1)$	$E_p(O_2)$	$E_p(R_1)$	$E_p(R_2)$	$\lvert i_{pO1}/i_{pR1} \rvert$
2	1.13*	1.56	–0.44*	–0.54	1.01
3-Cl	1.37	/	–0.42*	-	1.15
3-Br	1.35	/	–0.37*	-	1.05
4	1.05	1.35*	–0.44*	-	-
5	1.04	1.36*	–0.46*	-	-

* Reversible or partially reversible.

In the negative potential scan, all complexes exhibit a quasi-reversible reductive response attributed to the tetrazine core as electroactive moiety.[20] As previously mentioned, this species is easy to reduce and the reduction is clearly even facilitated in the palladium complexes, as evidenced by the positive shift of $E_p(R_1)$ between **1** (–0.87 V *vs* SCE, Figure 5) and the coordinated *s*-diphenyltetrazine in the complexes observed from –0.37 V to –0.46 V *vs* SCE (Table 1). A variation comprised between +0.41 and +0.50 V, is thus observed depending on the complex. This suggests also that the coordination of the *s*-diphenyltetrazine induces a lowering of the energy for the lower unoccupied molecular orbital (LUMO). Notably, for the dimeric palladacycle **2**, the single reduction peak is split in two, as a consequence of a significant electronic interaction existing between the two Tz moieties. This interaction is believed to naturally operate "through space" if these two moieties are facing each other while being maintained at short distance by the bridged dipalladium system.[21]

Regarding the oxidative reactivity, when operating in the positive potential scan direction, no response is observed for **1**, whereas, for the complexes **2**, **3-Cl**, **3-Br**, two or one peaks are present (Figure 5). These are attributable to the oxidation of the Pd(II) center. For dinuclear **2** the first oxidation potential (1.13 V *vs* SCE) is slightly less positive than the oxidation for mononuclear complexes **3-Cl** (1.37 V *vs* SCE) and **3-Br** (1.35 V *vs* SCE) resulting in $\Delta E_p(O_1)$ = –0.24 and –0.22 V, respectively (Table 1). This is a trend already encountered between dimeric and monomeric complexes possessing the same ligand environment.[22] The voltammetric behaviour of the dinuclear palladium complexes with *N*-containing heterocyclic ligands has been previously explored.[23] There is no general agreement on the number of electrons transferred at each of the two distinct oxidation peaks. Indeed, these are associated with either one-electron transitions, $Pd^{II}/Pd^{II} \rightarrow Pd^{III}/Pd^{II}$ followed by another $Pd^{III}/Pd^{II} \rightarrow Pd^{III}/Pd^{III}$ (case **a**), or two-electron transitions $Pd^{II}/Pd^{II} \rightarrow Pd^{III}/Pd^{III}$ and then a $Pd^{III}/Pd^{III} \rightarrow Pd^{IV}/Pd^{IV}$ (case **b**). Herein, the oxidation process for **2** seems to be associated with two Pd^{II} centers sequentially oxidized at the +III state (case **a**),[24] based on the internal calibration provided by the reduction process (peak intensity in relation with n_{e^-} equal to 1 per each Tz unit).

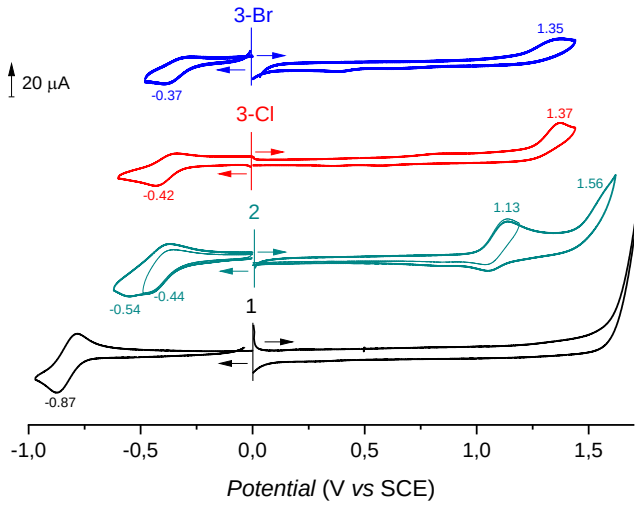

Figure 5. Cyclic voltammograms of **1** (black), [**2**] (green), [**3-Cl**] (red), [**3-Br**] (blue) in DMF (0.1 M), $TEABF_4$, (10^{-3} M), v = 100 mV.s^{-1}, WE: GCE (Ø = 2 mm).

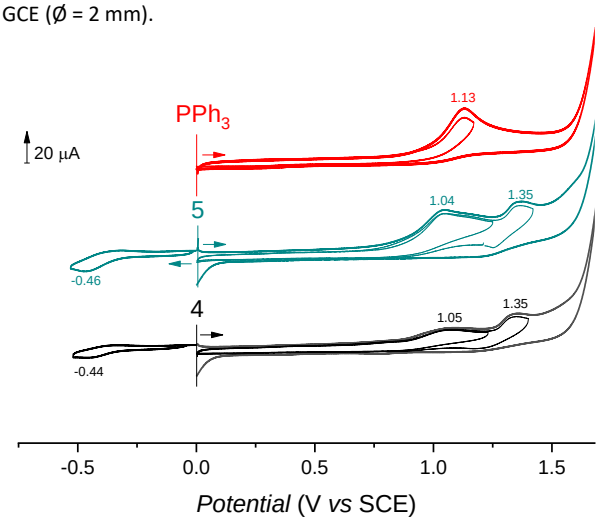

Figure 6. Cyclic voltammograms of [**4**] (black), [**5**] (green), PPh_3 (red) in DMF (0.1 M) $TEABF_4$ (10^{-3} M), v = 100 mV.s^{-1}, WE: GCE (Ø = 2 mm).

The mononuclear complexes **3-Cl** and **3-Br** displayed a single oxidation peak at close potential $E_p(O_1)$ = 1.37 and 1.35 V, respectively (Figure 5). This corresponds to a single-electron transfer by comparison with the reduction peak intensity that was observed in the one-electron reduction of the Tz core (see $E_p(R_1)$ = –0.42 and –0.37 V, respectively). Consequently, the oxidation process for **3-Cl** and **3-Br** results in the conversion of their Pd^{II} center into a Pd^{III} center.

The phosphino complexes **4** and **5** were studied in the same conditions of solvent and supporting electrolyte. On the oxidation side, for both **4** and **5**, two oxidation peaks are observed at nearly the same potentials (1.04 and 1.05 V and 1.35 V for both, Figure 6). The first irreversible step seems to concern the phosphine as electroactive moiety. Indeed, uncoordinated PPh_3 is oxidized at a close potential range of 1.13 V. For both complexes, the second step is reversible and its potential at 1.35 V is similar to the potential of **3-Cl** (1.37 V). This strongly suggests that a Pd(III) complex of similar structure may form at this stage, with a solvent molecule replacing the pyridine, assuming that PPh_3 was released at the first oxidation step.

Oxidation at the electrolysis scale.

To better assess the pertinence of these complexes as intermediates in Pd-catalyzed C–X bond formation on *s*-aryltetrazines, the CV

studies were extended at the bulk electrolysis scale (Scheme 4). Halogenated dimeric palladacycles have very limited solubility whatever the solvent tested which limited their studies by electrochemistry. Dichloromethane was found appropriate for **3-Cl** and acetonitrile adequate for **3-Br**, each being used in the presence of pyridine (1% v/v). By using a three-electrode configuration, the electrolyses of **3-Cl** and **3-Br** were achieved on platinum as electrode material and at fixed potential (E_{app} = 1.10 and 0.93 V *vs* SCE, for **3-Cl** and **3-Br**, respectively). For both compounds, a full conversion was obtained for a charge equivalent to nearly 2 equiv. of e^- per **3-X** unit (Table 2). Afterwards, in both cases, the C–X coupling products **1a-X** (Scheme 4) were identified and isolated in *ca* 50% yield (Table 2).

In the case of the reaction of Scheme 4, a Pd(IV) intermediate can be reasonably postulated, taking into account the two-electrons transfer occurring in these electrolysis experiments. This would be consistent with the reported electrochemical oxidation of a sp^3-C–H to C–O acetoxylation from a 8-methylquinolino-Pd(II) acetate complex via a Pd(IV) intermediate.[25]

The successful stoichiometric electrochemical oxidation of the *ortho*-metallated complexes **3-X**, which lead to the formation of C–X bonds from a reductive elimination process, encouraged us to investigate the synthesis of *ortho*-halogenated *s*-diphenyltetrazine by a Pd-electrocatalyzed functionalization pathway.

Direct C–H halogenation of s-diphenyltetrazine 1 by electrocatalysis. We initiated our studies by C–H halogenation attempts using the mild conditions reported by Kakiuchi group, with an H-type divided cell. However, contrary to their cell that was equipped with a non-conventional anion exchange membrane, we used a H-type cell with two compartments divided by classic fine glass frit.[7-10] The chlorination was performed with **1** in DMF using 10 mol% of $PdCl_2$ in the anodic compartment and 2 M solution of hydrogen chloride as supporting electrolyte and nucleophilic reagent. Under these electrosynthesis conditions no chlorination was observed at 90 °C at 10 mA.

The reaction was then attempted with **1** using 10 mol% of $PdCl_2$ in AcOH at 100 °C, with lithium chloride (10 equiv.) as the chlorinated reagent, and KOAc (1 equiv) as the base (Table 3, top), with the view to favor the formation of the palladacycle intermediate. The results of these so-called "standard condit ions" are reported in Table 3, entry 1.

Scheme 4. Electrochemical oxidation of complexes 3-X (X = Cl, Br).

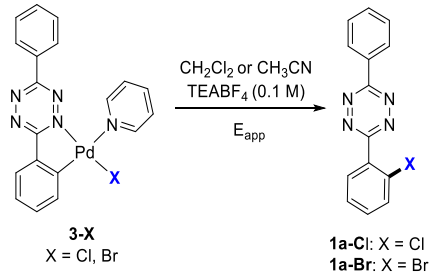

Table 2. Conditions and results for the electrolysis of complexes **3-X**.

Entry	**3-X**	Solvent	E_{app} (V)	Charge (F)	Isolated yield (%)
1	**3-Cl**	CH_3CN	1.10 V	2.3	**1a-Cl**: 46
2	**3-Br**	CH_2Cl_2	0.93 V	2.0	**1a-Br**: 56

[**3-X**] = 10^{-3} M, $TEABF_4$ (0.1 M), working electrode: Pt, divided cell.

Table 3. Pd-electrocatalyzed *o*-C–H halogenation of *s*-diphenyltetrazine (**1**).

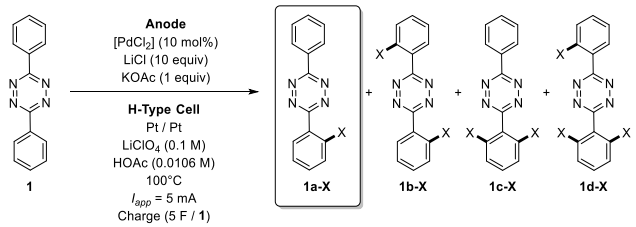

Entry	Changes from the "standard conditions"	Conv. (%)	1a-X (%)	1b-X (%)	1c-X (%)	1d-X (%)
1	none	43	38 (37)	5	-	-
2	no $PdCl_2$	17	nd	-	-	-
3	no LiCl	20	20 (7)	-	-	-
4	no KOAc	17	17 (nd)	-	-	-
5	DMF instead of HOAc	0	-	-	-	-
6	10 instead of 5 F	94	41 (9)	36 (8)	17	trace
7	120 instead of 100 °C	98	28 (17)	40 (20)	14	16 (8)
8	With PPh_3 (10%)	47	41	5	1	trace
9	5 equiv Li**Br**	0	-	-	-	-
10	5 equiv Li**I**	21	21 (16)			
11	3 equiv $\mathbf{I_2}$	57	30 (12)	27 (10)		

[a] Standard conditions. H-Type divided cell. Anode: Pt, $LiClO_4$ (0.1 M), *s*-diphenyltetrazine **1** (0.2 mmol, 1 equiv), $PdCl_2$ (10 mol%), LiCl (10 equiv), KOAc (1 equiv) in HOAc (0.02 M) at 100 °C. Cathode: Pt, $LiClO_4$ (0.1 M), in HOAc (0.02 M) at 100 °C. Applied current: 5 mA. Conversion based on ^{1}H NMR ($CDCl_3$). Isolated yields based on the starting diphenyltetrazine **1** are under brackets. nd: not determined.

The electrolysis was performed with 5 mA current and stopped after abstraction of 5 F per mol of **1**. Pleasingly, the targeted catalytic halogenation was successful. Nevertheless, the *s*-diphenyl tetrazine **1** confirmed to be a challenging substrate in terms of C–H functionalization selectivity, since up to four halides were introduced in the available *ortho*-position of the Tz core (Table 3), and a mixture of compounds **1a-Cl** (38%) and **1b-Cl** (5%) was mainly obtained in the initial standard conditions.

In the absence of $PdCl_2$ no conversion to **1a-Cl** was observed (Table 3, entry 2). The yield of **1a-Cl** decreased significantly to 22% in the absence of LiCl (entry 3), and to 17% in the absence of the base KOAc (entry 4). In contrast to the conditions reported by Kakiuchi group (Figure 1) the C–H halogenation reaction does not occur in DMF (entry 5). We doubled the abstracted charge from 5 to 10 F of **1** (entry 6), which indeed led to a higher conversion from 44% (entry 1) to 94%. However, the chlorination reaction extended to the dichlorinated product **1b-Cl** (formed in 36% *vs* 41% for **1a-Cl**). The additional presence of trichlorinated **1c-Cl** (17%) and traces of tetrachlorinated **1d-Cl** hampered a proper purification, which resulted in poor isolated yields. This experiment highlighted the feasibility of polyhalogenation. A similar result with 98% conversion was obtained by increasing the temperature to 120 °C (entry 7), forming *in fine* a mixture of **1a-Cl** (28%), **1b-Cl** (40%), **1c-Cl** (14%) and **1d-Cl** (16%). These results confirmed that the selectivity decreases as the conversion increases. Because of the purification issue, a lower conversion rate allowed to reach higher preparative yield of the monohalogenated product **1a-Cl**. The addition of 10% mol of

PPh_3, in order to generate in situ the complex **4**-Cl during the electrocatalysis, was also attempted (entry 8). Similar results were obtained as in our standard conditions (entry 1 vs. entry 8) and the triphenylphosphine was found oxidized after reaction. We assume that the phosphine is released from the palladacycle during the electrocatalysis and replaced by a second tetrazine. If occuring at the beginning of the reaction, the active catalyst could be the same thus inducing no significant difference between these two experiments, both in conversion and selectivity. This assumption is in agreement with the voltammetric behavior of **4-Cl** (see above) for which the decoordination of PPh_3 seems to be the immediate reaction expressed at the first oxidation step.

The electrochemical C–H activation/functionalization of **1** was extended using brominating and iodinating agents. The use of 5 equiv. of LiBr (entry 9) failed to provide any conversion. Conversely, the reaction using 5 equiv. of LiI led to 21% of **1a-I** (16% isolated yield, entry 10). The reaction achieved with I_2 improved the conversion up to 57% of **1a-I** (entry 11) with synthetic access to **1b-I** also achieved (27%).

Based on these results and previous studies,[12b,26] tentative mechanisms of the electrocatalyzed halogenation of *s*-diphenyltetrazine are proposed in Scheme 5. In the first mechanism pathway, a direct electron transfer from the palladacycle occurs leading to the generationof a Pd(IV) intermediate. Then, the reductive elimination leads to the formation of the halogenated tetrazine (Scheme 5, a). This postulate is in agreement with the electrochemical oxidation of our complexes **3-X** (Scheme 4). Nevertheless, the formation of the active halonium ion at the anode which oxidize the palladium cannot be ruled out (Scheme 5, b). The fact that the palladium-electrocatalyzed bromination reaction did not occur (table 3, entry 8) while the electro-oxidation of the corresponding palladacycle **3-Br** proceeds (table 2, entry 2) does not allow us to exclude these second way or the coexistence of the two mechanisms during the electrocatalysis.

Scheme 5. Catalytic cycle proposals for the electrocatalyzed halogenation of *s*-tetrazine.

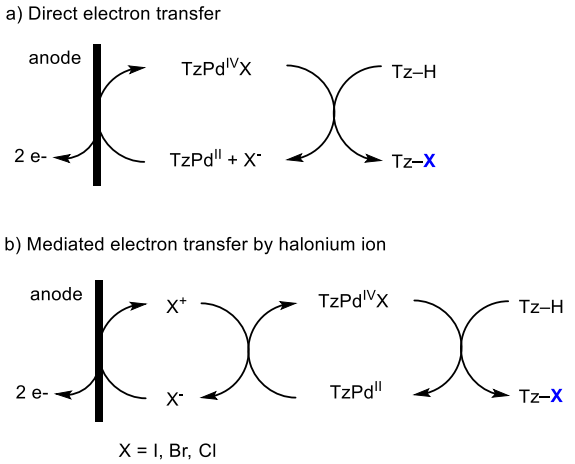

■ CONCLUSION

We reported the first electrochemical palladium-catalyzed halogenation of C–H bonds on redox active *s*-tetrazine platform. The electrochemical oxidation of preformed and fully characterized tetrazine-palladacycles demonstrated that they are key intermediates of the transformation during the catalytic cycle.

■ EXPERIMENTAL SECTION

General Procedures. All reagents were purchased from commercial suppliers and used without purifications. All reactions were performed in Schlenk tubes. ^{1}H (500 MHz), ^{13}C (125 MHz), ^{31}P (202 MHz) spectra were recorded on Brucker AVANCE NEO instrument. Chemical shifts are reported in ppm relative to $CDCl_3$ (^{1}H: 7.26 and ^{13}C: 77.16) or CD_2Cl_2 (^{1}H: 5.32 and ^{13}C: 54.00) and coupling constants *J* are given in Hz. High resolution mass spectra (HRMS) were obtained on a ThermoFischer ISQ-EM with ESI source. Elemental analysis experiments were performed Thermo Electron Flash EA 1112 Series.

Cyclic voltammetry measurements: All manipulations were performed using Schlenk techniques in an atmosphere of dry oxygen-free argon at room temperature (T = 20 °C ± 3 °C). The supporting electrolyte, tetraethylammonium hexafluoroborate ($TEABF_4$), was degassed under vacuum before use and then dissolved to a concentration of 0.1 mol.L^{-1}.

Voltammetric analyses were carried out in a standard three-electrode cell, with Biologic SP-300 potentiostat, connected to an interfaced computer that employed EC-Lab (v. 11.25) software. The reference electrode was a saturated calomel electrode (SCE) separated from the analyzed solution by a sintered glass disk filled with the background solution (V = 5 ml). The auxiliary electrode was a platinum foil separated from the analyzed solution by a sintered glass disk filled with the background solution (V = 5 ml). For all voltammetric measurements, the working electrode was a glassy carbon disk working electrode (Ø = 2 mm) or a platinum electrode (Ø = 1.6 mm) dipped in the compartment (V = 5 ml).

Bulk electrolyses: Electrolyses were performed under argon in HOAc (0.1 M $LiClO_4$) at applied current (5 mA) in a H-type cell equipped with a magnetic stirring bar (two compartments separated with glass frits of medium porosity) with an Autolab PGSTAT 302 N potentiostat, connected to an interfaced computer that employed Electrochemistry Nova software. One platinum wire spiral (l = 50 cm, Ø = 1 mm, Stot ≈ 15 cm^2) was used as working electrode, another platinum wire spiral (l = 50 cm, Ø = 1 mm, Stot ≈ 15 cm^2) was used as the counter electrode.

Synthesis of the Palladacycles.

Synthesis of 2: To a Schlenk flask containing palladium acetate (85 mg, 0.38 mmol, 1 equiv) and **1** (89 mg, 0.38 mmol, 1 equiv) was added acetic acid (55 ml, [6.9 mM/(**1**)]). After heating at 80°C under argon for 14 h, the green solution was concentrated under vacuum. The crude mixture was dissolved in dichloromethane and then was filtrated through a pad of celite (with dichloromethane). The solvent was removed under *vacuum* and the mixture was recrystallized in dichloromethane/heptane mixture to afford **2** as a dark green solid (108 mg, 71% yield). ^{1}H NMR (500 MHz, CD_2Cl_2): δ (ppm) = 8.38 (d, *J* = 8.2 Hz, 4H), 7.72 (t, *J* = 7.9 Hz, 2H), 7.69–7.61 (m, 6H), 6.92–6.87 (m, 4H), 6.53–6.47 (m, 2H), 2.33 (s, 7H). ^{13}C NMR (125 MHz, $CDCl_3$): δ (ppm) = 181.8, 170.3, 162.9, 154.4, 134.4, 133.3, 132.7, 131.5, 130.9, 129.5, 127.9, 126.9, 125.8, 53.4, 24.4. Elemental analysis: Calcd (%) for $C_{32}H_{24}N_8O_4Pd_2$ (795.99): C 48.20, H 3.03, N 14.04; Found: C 47.57, H 2.72, N 13.66. HRMS + p ESI (m/z) [M+Na]$^+$ Calcd for $C_{32}H_{24}N_8O_4Pd_2Na$: 818.98824; Found: 818.99184.

Synthesis of 3-Cl: LiCl (10 mg, 0.25 mmol, 10 equiv) was added to a solution of **2** (20 mg, 0.025 mmol, 1 equiv) in chloroform (10 ml, [2.5 mM/(**2**)]). The initial green solution turned to a pale orange solution. After stirring for 2 h at room temperature, the solvent was removed under vacuum and then dichloromethane was added for a better solubility (10 ml, [2.5 mM/(**2**)]). Pyridine (4 µl, 0.05 mmol, 2 equiv) was then added, and the solution was stirred for 2 h giving a bright orange solution. The solution was washed with water and then the product was recrystallized in dichloromethane/heptane to afford **3-Cl** as an orange solid (14 mg, 61% yield). ^{1}H NMR (500 MHz, CD_2Cl_2): δ (ppm) = 8.90 (bs, *J* = 5.3 Hz, 2H), 8.18–8.12 (m, 4H), 7.97 (t, *J* = 7.8 Hz, 1H), 7.62 (t, *J* = 7.5 Hz, 1H), 7.56–7.52 (m, 4H), 7.34 (td, *J* = 7.6,

1.6 Hz, 1H), 7.29 (td, *J* = 7.3, 1.2 Hz, 1H). ^{13}C NMR (125 MHz, CD_2Cl_2): δ (ppm) = 171.9, 163.5, 155.4, 151.5, 138.4, 137.1, 136.2, 133.2, 130.9, 129.4, 127.6, 126.1, 124.7. Elemental analysis: Calcd (%) for $C_{19}H_{14}ClN_5Pd$ (452.99): C 50.24, H 3.11, N 15.42; Found: C 50.80, H 2.94, N 13.71. HRMS + p ESI (m/z) $[M+Na]^+$ Calcd for $C_{19}H_{14}ClN_5PdNa$: 452.99724; Found: 452.99791.

Synthesis of 3-Br: LiBr (22 mg, 0.25 mmol, 10 equiv) was added to a solution of **2** (20 mg**,** 0.025 mmol, 1 equiv) in chloroform (10 ml, [2.5 mM/(**2**)]). The initial green solution turned to red. After stirring for 30 min at room temperature, the solvent was removed under vacuum and then dichloromethane was added for a better solubility (10 ml, [2.5 mM/(**2**)]). Pyridine (4 µl, 0.05 mmol, 2 equiv) was then added, and the solution was stirred for 30 min giving an orange solution. The solution was washed with water and then the product was recrystallized in dichloromethane/heptane to afford **3-Br** as an orange solid (21 mg, 83% yield). ^{1}H NMR (500 MHz, CD_2Cl_2): δ (ppm) = 8.90 (bs, 2H), 8.31 (d, *J* = 7.47 Hz, 1H), 8.12–8.06 (m, 3H), 7.94 (t, *J* = 8.1 Hz, 1H), 7.61 (t, *J* = 7.4 Hz, 1H), 7.53–7.51 (m, 4H), 7.23–7.16 (m, 2H). ^{13}C NMR (125 MHz, CD_2Cl_2): δ (ppm) = 123.9, 125.3, 126.4, 126.9, 128.3, 128.7, 128.7, 129.9, 130.0, 130.9, 132.5, 133.8, 136.6, 151.2, 152.7, 163.5. Elemental analysis: Calcd (%) for $C_{19}H_{14}BrN_5Pd$ (496.94): C 45.76, H 2.83, N 14.04; Found: C 41.68, H 2.32, N 11.94. HRMS + p ESI (m/z) $[M-Br]^+$ Calcd for $C_{19}H_{14}N_5Pd^+$: 418.02840. Found: 418.02773.

Synthesis of 4: LiCl (10 mg, 0.25 mmol, 10 equiv) was added to a solution of **2** (20 mg, 0.025 mmol, 1 equiv) in chloroform (10 ml, [2.5 mM/(**2**)]). The initial green solution turned to a pale orange solution. After stirring for 2 h at room temperature, the solvent was removed under vacuum and then dichloromethane was added for a better solubility (10 ml, [2.5 mM/(**2**)]). PPh_3 (13 mg, 0.05 mmol, 2 equiv) was added and the solution was stirred for 2 h giving a bright orange solution. The solution was washed with water then the product was recrystallized by dichloromethane/heptane to give an orange crystal (20 mg, 61% yield). ^{1}H NMR (500 MHz, CD_2Cl_2): δ (ppm) = 8.73 (dd, *J* = 6.8, 3.0 Hz, 2H), 8.29 (d, *J* = 7.29 Hz, 1H), 7.81–7.77 (m, 6H), 7.69–7.61 (m, 3H), 7.52–7.49 (m, 3H), 7.43–7.40 (m, 6H), 7.15 (t, *J* = 7.4 Hz, 1H), 6.80–6.77 (td, *J* = 7.6, 1.7 Hz, 1H), 6.67 (d, *J* = 7.9 Hz, 1H). ^{31}P NMR (202 MHz, CD_2Cl_2): δ (ppm) = 42.9. ^{13}C NMR (125 MHz, CD_2Cl_2): δ (ppm) = 125.4, 128.1, 128.2, 128.3, 129.5, 130.4, 130.7, 131.0, 131.4, 132.4, 133.2, 135.3, 135.4, 138.8. Elemental analysis: Calcd (%) for $C_{32}H_{24}ClN_4PPd$ (636.04): C 60.30, H 3.80, N 8.79; Found: C 57.17, H 3.37, N 8.22. HRMS + p ESI (m/z) $[M-Cl]^+$ Calcd for $C_{32}H_{24}N_4PPd$: 601.07679; Found: 601.07850.

Synthesis of 5: PPh_3 (8 mg, 0.03 mmol, 1 equiv) was added to a solution of **4** (20 mg, 0.03 mmol, 1 equiv) in dichloromethane (10 ml, [3 mM/(**4**)]) at room temperature and stirred for 20 min. The solvent was removed under vacuum and the crude was recrystallized in dichloromethane/heptane to yield a purple solid (25 mg, 88% yield). ^{1}H NMR (500 MHz, CD_2Cl_2): δ (ppm) = 8.73 (dd, *J* = 6.7, 3.0 Hz, 2H), 7.71–7.67 (m, 4H), 7.46–7.42 (m, 13H), 7.34–7.30 (m, 6H), 7.22–7.19 (m, 12H), 6.75 (td, *J* = 7.5, 1.2 Hz, 1H), 6.61 (td, *J* = 7.4, 1.6 Hz, 1H). ^{31}P NMR (202 MHz, CD_2Cl_2): δ (ppm) = 21.9. ^{13}C NMR (125 MHz, CD_2Cl_2): δ (ppm) = 164.2, 163.9, 162.2, 137.0, 135.2, 134.4, 132.4, 132.3, 130.9, 129.8, 129.4, 129.3, 127.8, 127.5, 123.1. Elemental analysis: Calcd (%) for $C_{50}H_{39}ClN_4P_2Pd$ (898.13): C 66.75, H 4.37, N 6.23; Found: C 66.93, H 4.71, N 5.63. HRMS + p ESI (m/z) $[M-Cl]^+$ Calcd for $C_{50}H_{39}N_4P_2Pd$: 863.16793; Found: 863.16808.

General procedure of palladium-electrocatalyzed functionalization of 3,6-diaryl-1,2,4,5-tetrazine, 1a-X.

As a typical experiment, *s*-aryltetrazine **1** (50 mg, 0.21 mmol, 1 equiv), LiX (2.1 mmol, 10 equiv), $PdCl_2$ (3.78 mg, 10 mol%), KOAc (21 mg, 0.21 mmol, 1 equiv) were introduced in the anodic compartment of a H-type cell and were degassed under *vacuum*. Under argon atmosphere, 10 ml ([0.02 M/(**1**)**]**) of the electrolyte solution ($LiClO_4$ in HOAc [0.1 M]) was added to each compartment, and the reaction mixture was heated at 100 °C. Electrolysis was stopped after an uptake of 5 or 10 F per tetrazine. After cooling down to room temperature, the reaction mixture was diluted with dichloromethane, and washed with water. The solvent was removed under vacuum and the residue was analyzed by ^{1}H NMR to determine the conversion. Finally, the crude product was purified by silica gel column chromatography using an appropriate ratio of the eluent (dichloromethane/heptane).

3-(2-chlorophenyl)-6-phenyl-1,2,4,5-tetrazine, 1a-Cl. Rf = 0.45 (dichloromethane/heptane = 1:1 (v/v)) as a purple solid. ^{1}H NMR (500 MHz, $CDCl_3$): δ (ppm) = 8.72–8.70 (m, 2H), 8.06 (dd, *J* = 7.50, 2.00 Hz, 1H), 7.70–7.62 (m, 4H), 7.58–7.51 (m, 2H).

3,6-bis(2-chlorophenyl)-1,2,4,5-tetrazine, 1b-Cl. Rf = 0.38 (dichloromethane/heptane = 1:1 (v/v)) as a purple solid. ^{1}H NMR (500 MHz, $CDCl_3$): δ (ppm) = 8.12 (dd, *J* = 7.50, 2.00 Hz, 2H), 7.65 (dd, *J* = 7.80, 1.50 Hz, 2H), 7.59–7.52 (m, 4H).

3-(2,6-dichlorophenyl)-6-(2-chlorophenyl)-1,2,4,5-tetrazine, 1c-Cl. Rf = 0.45 (dichloromethane/heptane = 1:1 (v/v)) as a purple solid.

^{1}H NMR (300 MHz, $CDCl_3$): δ (ppm) = 8.15–8.11 (m, 1H), 7.67–7.61 (m, 1H), 7.59–7.49 (m, 5H).

3-(2-bromophenyl)-6-phenyl-1,2,4,5-tetrazine, 1a-Br. Rf = 0.43 (dichloromethane/heptane = 1:1 (v/v)) as a purple solid. ^{1}H NMR (300 MHz, $CDCl_3$): δ (ppm) = 8.73–8.69 (m, 2H), 8.02 (ddd, *J* = 7.49, 1.93, 0.23 Hz, 1H), 7.82 (ddd, *J* = 7.94, 0.99, 0.30 Hz, 1H), 7.70–7.60 (m, 3H), 7.57 (td, *J* = 8.06, 0.52 Hz, 1H), 7.47 (ddd, *J* = 7.96, 7.54, 1.80 Hz, 1H).

3-(2-iodophenyl)-6-phenyl-1,2,4,5-tetrazine, 1a-I. Rf = 0.44 (dichloromethane/heptane = 1:1 (v/v)) as a purple solid. ^{1}H NMR (300 MHz, $CDCl_3$): δ (ppm) = 8.74–8.70 (m, 2H), 8.12 (dd, *J* = 7.97, 0.95 Hz, 1H), 7.99 (dd, *J* = 7.74, 1.60 Hz, 1H), 7.70–7.58 (m, 4H), 7.31–7.26 (m, 1H).

■ ASSOCIATED CONTENT

Supporting Information.

The supporting Information is available free of charge on the ACS Publications website at DOI:---

Experimental procedures, voltammetry analysis and spectral data (^{1}H, ^{19}F, ^{13}C) for all new compounds, (PDF) and crystallographic data (CIF). CCDC numbers: 2221614 (**3-Cl)**, 2221615 (**4**), 2221616 (**5**) contain the supplementary crystallographic data for this paper. These data can be obtained free of charge from The Cambridge Crystallographic Data Centre.

■ AUTHOR INFORMATION

Corresponding Authors

*E-mail:

Julien.roger@u-bourgogne.fr

Jean-cyrille.hierso@u-bourgogne.fr

Dominique.lucas@u-bourgogne.fr

ORCID

Asmae Bousfiha: 0000-0002-0860-3469

Helene Cattey: 0000-0002-4416-7510

Paul Fleurat-Lessard: 0000-0003-3114-2522

Charles H. Devillers: 0000-0001-9078-7035

Dominique Lucas: 0000-0002-9639-132X

Jean-Cyrille Hierso: 0000-0002-2048-647X

Julien Roger: 0000-0002-4964-366X

Notes

The authors declare no competing financial interest.

■ ACKNOWLEDGMENTS

This work was supported by the CNRS, the Université de Bourgogne,

the Conseil Régional Bourgogne Franche-Comté and the Fonds Européen de Développement Régional (FEDER). This work was also funded by the French Agence Nationale de la Recherche *via* the ANR-JCJC program 2018 FIT-FUN (ANR-18-CE07-0015, grant for AB) and the COMUE UBFC (I-SITE UB180013.MUB. IS_SmartTZ). Thanks are due to the PACSMUB platform for analyses (SATT SAYENS) especially M.-J. Penouilh, Q. Bonnin and T. Regnier.

■ REFERENCES

(1) (a) Dick, A. R.; Hull, K. L.; Sanford, M. S. A Highly Selective Catalytic Method for the Oxidative Functionalization of C−H Bonds. *J. Am. Chem. Soc.* **2004**, *126*, 2300–2301. (b) Neufeldt, S. R.; Sanford, M. S. Controlling Site Selectivity in Palladium-Catalyzed C–H Bond Functionalization. *Acc. Chem. Res.* **2012**, *45*, 936–946.

(2) Sambiagio, C.; Schönbauer, D.; Blieck, R.; Dao-Huy, T.; Pototschnig, G.; Schaaf, P.; Wiesinger, T.; Zia, M. F.; Wencel-Delord, J.; Besset, T.; Maes, B. U. W.; Schnürch, M. A Comprehensive Overview of Directing Groups Applied in Metal-catalysed C–H Functionalization Chemistry. ***Chem. Soc. Rev.***, **2018**, ***47***, 6603–6743.

(3) Kingston, C.; Palkowitz, M. D.; Takahira, Y.; Vantourout, J. C.; Peters, B. K.; Kawamata, Y.; Baran, P. S. A Survival Guide for the "Electro-curious". *Acc. Chem. Res.* **2020**, *53*, 72–83.

(4) For recent reviews on electrocatalysis, see for instance: (a) Erchinger, J. E.; van Gemmeren, M. Electrochemical Methods for Pd-catalyzed C–H Functionalization. *Asian J. Org. Chem.* **2021**, *10*, 50–60. (b) Jiao, K.-J.; Xing, Y.-K.; Yang, Q.-L.; Qui, H.; Mei. T.-S. Site-Selective C−H Functionalization via Synergistic Use of Electrochemistry and Transition Metal Catalysis. *Acc. Chem. Res.* **2020**, *53*, 300–310; (c) Sauermann, N.; Meyer, T. H.; Qiu, Y.; Ackermann, L. Electrocatalytic C–H Activation. *ACS Catal.* **2018**, *8*, 7086−7103.

(5) (a) Petrone, D. A.; Ye, J.; Lautens, M. Modern Transition-Metal-Catalyzed Carbon–Halogen Bond Formation. *Chem. Rev.* **2016**, *116*, 8003−8104; (b) Das, R.; Kapur, M. Transition-Metal-Catalyzed Site-Selective C−H Halogenation Reactions. *Asian J. Org. Chem.* **2018**, *7*, 1524–1541.

(6) Kakiuchi, F.; Kochi, T.; Mutsutani, H.; Kobayashi, N.; Urano, S.; Sato, M.; Nishiyama, S.; Tanabe, T. Palladium-Catalyzed Aromatic C–H Halogenation with Hydrogen Halides by Means of Electrochemical Oxidation. *J. Am. Chem. Soc.* **2009**, *131*, 11310–11311.

(7) Aiso, H.; Kochi, T.; Mutsutani, H.; Tanabe, T.; Nishiyama, S.; Kakiuchi, F. Catalytic Electrochemical C–H Iodination and One-Pot Arylation by ON/OFF Switching of Electric Current. *J. Org. Chem.* **2012**, *77*, 7718−7724.

(8) Konishi, M.; Tsuchida, K.; Sano, K.; Kochi, T.; Kakiuchi, F. Palladium-Catalyzed *ortho*-Selective C–H Chlorination of Benzamide Derivatives under Anodic Oxidation Conditions. *J. Org. Chem.* **2017**, *82*, 8716−8724.

(9) Sano, K.; Naoki, K.; Kochi, T.; Kakiuchi, F. Palladium-Catalyzed C–H Iodination of *N*-(8-Quinolinyl)benzamide Derivatives Under Electrochemical and Non-Electrochemical Conditions. *Asian J. Org. Chem.* **2018**, *7*, 1311–1314.

(10) Yang, Q.-L.; Wang, X.-Y.; Wang, T.-L.; Yang, X.; Liu, D.; Tong, X.; Wu, X.-Y.; Mei, T.-S. Palladium-Catalyzed Electrochemical C–H Bromination Using NH_4Br as the Brominating Reagent. *Org. Lett.* **2019**, *21*, 2645–2649.

(11) For an overview, see: (a) Clavier, G.; Audebert, P. *s*-Tetrazines as Building Blocks for New Functional Molecules and Molecular Materials. *Chem. Rev.* **2010**, *110,* 3299–3314. (b) Lipunova, G. N.; Nosova, E. V.; Zyryanov, G. V.; Charushin, V. N.; Chupakhin, O. N. 1,2,4,5-Tetrazine Derivatives as Components and Precursors of Photo- and Electroactive Materials. *Org. Chem. Front.*, **2021**, *8*, 5182–5205. (c) Choi, S.-K.; Kim, J.; Kim, E. Overview of Syntheses and Molecular-Design Strategies for Tetrazine-Based Fluorogenic Probes. *Molecules* **2021**, *26*, 1868–1884.

(12) (a) Testa, C.; Gigot, E.; Genc, S.; Decreau, R.; Roger, J.; Hierso, J.-C. *Ortho*-Functionalized Aryl Tetrazines by Pd-Catalyzed Direct C–H Halogenation: Application to Fast Electrophilic Fluorination Reactions. *Angew. Chem. Int. Ed.* **2016**, *55*, 5555−5559; (b) Mboyi, C. D.; Testa, C.; Reeb, S.; Genc, S.; Cattey, H.; Fleurat-Lessard, P.; Roger, J.; Hierso, J.-C. Versatile Tuning of *N*-directed Palladium C–H Halogenation Building Diversity in *ortho*-Substituted *s*-Aryltetrazines. Hierso *ACS Catal.* **2017**, *7*, 8493–8501; (c) Daher, A.; Abidi, O.; Hierso, J.-C.; Roger, J. Alkali Halides as Nucleophilic Reagent Source for *N*-Directed Palladium-Catalysed *ortho*-C–H Halogenation of *s*-Tetrazines and Other Heteroaromatics. *RSC Adv.* **2022**, *12*, 30691–30695.

(13) (a) Mboyi, C. D.; Vivier, D.; Daher, A.; Fleurat-Lessard, P.; Cattey, H.; Devillers, C. H.; Bernhard, C.; Denat, F.; Roger, J.; Hierso, J.-C. Bridge Clamp Bis-Tetrazines Stacked by [N]8-π-Interactions and Azido-s-Aryl Tetrazines: New Classes of Doubly Clickable Tetrazines. *Angew. Chem. Int. Ed.* **2020**, *59*, 1149–1154; (b) Mboyi, C. D.; Daher, A.; Khirzada, N.; Devillers, C. H.; Cattey, H.; Fleurat-Lessard, P.; Roger, J.; Hierso, J.-C. Synthesis and Structural Characterisation of Bulky Heptaaromatic (Hetero)aryl o-Substituted *s*-Aryltetrazines. *New J. Chem.* **2020**, *44*, 15235–15243.

(14) (a) Dupont, J.; Consorti, C. S.; Spencer, J. The Potential of Palladacycles: More Than Just Precatalysts. Chem. Rev. ***2005****, 105, 2527–2571. (b) Dastbaravardeh, N.; Christakakou, M.; Haider, M.; Schnürch, M. Recent Advances in Palladium-Catalyzed Csp3–H Activation for the Formation of carbon–carbon and carbon-heteroatom bonds. Synthesis* ***2014****, 46, 1421–1439; (c) Beleskaya, I. P.; Cheprakov, A. V. Palladacycles in catalysis – A Critical Survey. J. Organomet. Chem.* ***2004****, 689, 4055–4082. (d) R. B. Bedford Palladacyclic Catalysts in C–C and C–Heteroatom Bond-Forming Reactions. Chem. Commun.,* ***2003****, 1787–1796.*

(15) Canty, A. J.; Ariafard, A.; Sanford, M. S.; Yates, B. F. Reactivity of Diaryliodine(III) Triflates toward Palladium(II) and Platinum(II): Reactions of $C(sp_2)$−I Bonds to Form Arylmetal(IV) Complexes; Access to Dialkyl(aryl)metal(IV), 1,4-Benzenediyl-Bridged Platinum(IV), and Triphenylplatinum(IV) Species; and Structural Studies of Platinum(IV) Complexes. *Organometallics*. **2013**, *32*, 544−555.

(16) Slater, J. W.; Rourke, J. P. Cyclometallated Nitrogen Heterocycles. *J. Organomet. Chem.*, **2003**, *688*, 112–120.

(17) (a) Structurally, two stereoisomers could be obtained, identified as *trans* (C^N^1 Pd-*ortho*-metallation with the first Tz and C^N^2 with the second Tz) and *cis* isomers (C^N^1 Pd-*ortho*-metallation from both Tz). However, the *trans* configuration is favored for reported dimeric analogs: out of 293 dimers structures reported in the Cambride Database, only 4 correspond to *cis* isomers. (b) One of the first Pd dimer with bridging acetate characterized by XRD was published in 1980: it was a *trans* isomer. Churchill, M. R.; Wasserman, H. J.; Young, G. J. Cyclometalation of 2-*p*-Tolylbenzthiazole and 2-*p*-Tolylbenzoxazole with Palladium(II) Acetate. Synthesis and Crystal Structures of the Acetate-Bridged Dimers $[(MeC_6H_3C_7H_4NS)Pd]_2(\mu\text{-}O_2CMe)_2$ and $[(MeC_6H_3C_7H_4NO)Pd]_2(\mu\text{-}O_2CMe)_2$. *Inorg. Chem.* **1980**, *19*, 762–770. (c) The first solid state structure of a *cis* isomer was published more than 20 years later: Fernández, A.; Vázquez-García, D.; Fernández, J. J.; López-Torres, M.; Suárez, A.; Castro-Juiz, S.; Vila, J. M. The First Crystal and Molecular Structure of a Syn-Acetato-Bridged Dinuclear Cyclometallated Complex $[Pd\{2,3,4\text{-}(MeO)_3C_6HC(H)=NCH_2CH_2OH\}(\mu\text{-}OAc)]_2$. *Eur. J. Inorg. Chem.* **2002**, *2002*, 2389–2401.

(18) As models, the use of pyridine and phosphine give simpler complexes than the addition of a second tetrazine, for which mixtures of several regiosisomers are formed.

(19) (a) Anderson, G. K.; Cross, R. J.; Leaman, S. A.; Robertson, F. J.; Rycroft, D. S.; Rocamora, M. J. Conformation and Ligand Exchange Reactions of *trans*-$[PdCl(C_6H_4\text{-}2\text{-}N_2Ph)(PR_3)_2]$ and Related Complexes. *J. Organomet. Chem.*, **1990**, *388*, 221–231. (b) Kim, Y.-J.; Chang, X.; Han, J.-T.; Lim, M. S.; Lee, W. S. Cyclometallated Pd(II) Azido Complexes Containing 6-Phenyl-2,2-bipyridyl or 2-

Phenylpyridyl Derivatives: Synthesis and Reactivity Toward Organic Isocyanides and Isothiocyanates. *Dalton Trans.* **2004**, 3699–3708.
(20) (a) Audebert, P.; Sadki, S.; Miomandre, F.; Clavier, G.; Vernières, M. C.; Saoud, M.; Hapiot, P. Synthesis of New Substituted Tetrazines: Electrochemical and Spectroscopic Properties. *New J. Chem.,* **2004**, *28*, 387–392. (b) Gleiter, R.; Schehlmann, V.; Spanget-Larsen, J.; Fischer, H.; Neugebauer, F. A. Photoelectron spectra of disubstituted 1,2,4,5-tetrazines. *J. Org. Chem*., **1988**, *53*, 5756–5762. (c) Min, D. J.; Lee, K.; Park, H.; Kwon, J. E.; Park, S. Y. Redox Potential Tuning of *s*-Tetrazine by Substitution of Electron-Withdrawing/Donating Groups for Organic Electrode Materials. *Molecules* **2021**, *26*, 894–907.
(21) For Electron Transfer to and from Molecules Containing Multiple and Noninteracting Redox Centers, see: (a) Flanagan, J. B.; Margel, S.; Bard, A. J.; Anson, F. C. Electrochemical oxidation of poly(vinylferrocene). *J. Am. Chem. Soc.* **1978**, *100*, 4248–4253. (b) Alvarez, J.; Kaifer, A. E. Structural and pH Control on the Electronic Communication between Two Identical Ferrocene Sites. *Organometallics* **1999**, *18*, 5733–5734. (c) Cuadrado, I.; Casado, C. M.; Alonso, B.; Morán, M.; Losada, J.; Belsky, V. Dendrimers Containing Organometallic Moieties Electronically Communicated. *J. Am. Chem. Soc.* **1997**, *119*, 7613–7614.
(22) Dudkina, Y. B.; Kholin, K. V.; Gryaznova, T. V.; Islamov, D. R.; Kataeva, O. N.; Rizvanov, I. K.; Levitskaya, A. I.; Fominykh, O. D.; Balakina, M. Y.; Sinyashin, O. G.; Budnikova. Y. L. Redox Trends in Cyclometalated Palladium(II) Complexes. *Dalton Trans*., **2017**, *46*, 165–177.
(23) (a) Bercaw, J. E.; Durrell, A. C.; Gray, H. B.; Green, J. C.; Hazari, N.; Labinger, J. A.; Winkler, J. R. Electronic Structures of Pd^{II} Dimers. *Inorg. Chem.* **2010**, *49*, 1801–1810. (b) Nguyen, B. N.; Adrio, L. A.; Albrecht, T.; White, A. J. P.; Newton, M. A.; Nachtegaal, M.; Figueroa, S. J. A.; Hii, K. K. Electronic Structures of Cyclometalated Palladium Complexes in the Higher Oxidation States. *Dalton Trans*., **2015**, *44*, 16586–16591. (c) Dudkina, Y. B.; Mikhaylov, D. Y.; Gryaznova, T. V.; Tufatullin, A. I.; Kataeva, O. N.; Vicic, D. A.; Budnikova, Y. H. Electrochemical *Ortho*-Functionalization of 2-Phenylpyridine with Perfluorocarboxylic Acids Catalyzed by Palladium in Higher Oxidation States. *Organometallics*, **2013**, *32*, 4785–4792.
(24) Testa, C.; Roger, J.; Fleurat-Lessard, P.; Hierso, J.-C. Palladium-Catalyzed C-H Bond Electrophilic Fluorination: Mechanistic Overview and Supporting Evidences. *Eur. J. Org. Chem.* **2019**, 233–253.
(25) Shrestha, A.; Lee, M.; Dunn, A. L.; Sanford, M. S. Palladium-Catalyzed C–H Bond Acetoxylation via Electrochemical Oxidation. *Org. Lett.* **2018**, *20*, 204−207.
(26) Yang, Q.-L.; Li, Y.-Q.; Ma, C.; Fang, P.; Zhang, X.-J.; Mei, T.-S. Palladium-Catalyzed C(Sp3)-H Oxygenation via Electrochimical Oxidation. *J. Am. Chem. Soc.* 2017, 139, 8, 3293–3298.